Deposition of nickel nanoparticles onto aluminum powders using a modified polyol process

J.L. Cheng [a], H.H. Hng [a,*], H.Y. Ng [b], P.C. Soon [b], Y.W. Lee [b]

[a] School of Materials Science & Engineering, Division of Materials Science, Nanyang Technological University, Singapore 639798, Singapore
[b] DSO National Laboratories, 20 Science Park Drive, Singapore 118230, Singapore

A B S T R A C T

Aluminum is commonly used as fuel additive for propellants. The main limitation to its use lies in comparatively slow ignition and oxidation/combustion kinetics. Combustion performance of aluminized propellants can be improved through the use of Ni-coated Al particles. Nanoparticles, with its increased reactivity, also improve combustion performance. Hence, in this work, nano-sized Ni particles coated onto commercially available micron-sized Al powders using a modified polyol process were synthesized and evaluated. Ni-coated Al powders of various compositions produced by this method showed significant improvement in the oxidation kinetics as compared to untreated Al powders. The onset oxidation temperatures for the Ni-coated Al powders were found to be significantly reduced as compared to pure untreated Al. Other than the oxides, the intermetallic compound, Al_3Ni was also detected in the 10 wt% Ni–Al powders that were heated to temperature above 1050 °C.

© 2008 Elsevier Ltd. All rights reserved.

1. Introduction

Currently, aluminum is widely used as high-energy fuel in areas such as propellants. However, including Al in fuel compositions is accompanied by a number of undesired features. A critical problem is the ignition of Al particles. Due to the protective oxide (alumina) layer on the particle surface, Al typically ignites in oxidizing atmosphere only after heating up to temperatures close to the melting point of alumina at 2300 K [1]. In addition, agglomeration of Al particles in the propellant surface layer also leads to incomplete burning of Al particles and promotes slag formation [2]. All these adverse effects result in the limited realization of the energy potential of the fuel. Previous studies have shown that the use of Ni-coated Al particles improves the combustion performances of aluminized propellants. Coating Al particles with a thin (10–100 nm) film of nickel was found to reduce particle agglomeration during metallized propellant combustion [3,4]. In addition, Ni-coated Al particles are observed to ignite easier than original Al particles, and the ignition temperature in Ni–Al system is close to the melting point of Al [5–7]. A recent report also found that the addition of nano-Ni powders to Al-based composite propellant effectively raised the propellant's burning rate and improve its combustion characteristics [8].

In this work, we attempt to study the effects of combining these two factors to produce Al powders coated with nano-Ni particles. The nano-sized Ni particles will be synthesized using a modified polyol process using hydrazine as reducing agent [9,10], and deposited onto commercially available micron-sized Al particles at the same time. The aim of this work is to determine whether the combination of nano-particles and Ni coating will improve the combustion behavior of Al powders through thermal analysis studies.

2. Experimental procedures

Three sets of Al–Ni samples with bulk compositions of 5, 10 and 30 wt% Ni were prepared. The nominal composition of the powders was determined from the starting precursor compositions. Nickel(II) acetate tetrahydrate $(Ni(Ac)_2 \cdot 4H_2O)$ supplied from Sigma–Aldrich was dehydrated in an oven at 120 °C for 5 h prior to the experiment. The whole experiment consists of mainly two stages. In the first stage, the required amount of $Ni(Ac)_2$ and sodium hydroxide (NaOH supplied from Sigma–Aldrich in pellets form) were suspended in 250 ml of ethylene glycol. Ethylene glycol acts both as a solvent and as a particle surface protective agent to prevent severe agglomeration of the particles. The mixture was then heated up to 60 °C for 25 min and stirred using a mechanical stirrer. In the second stage, Al powders (99.5% purity supplied by Alfa Aesar of 325 mesh; average particle size 44–50 μm) was added into the mixture followed by the addition of hydrazine

hydrate (N₂H₄·H₂O supplied by Sigma–Aldrich equivalent to 64% hydrazine). This stage involves the nucleation and growth of the nickel particles from the ethylene glycol solution and deposited onto the Al particles; or by nucleating from the activation sites of the Al particles itself; or a combination of both. This process was allowed to proceed for 120 min at 60 °C. At the end of all reactions, the suspension was cooled to room temperature and the residue was separated from the solution and washed with acetone and ethanol several times. The collected powders were then dried in an oven at 80 °C for 12 h. All the chemicals used throughout the study were reagent grade in purity.

The modified polyol process involves the following steps: (1) formation of Ni(OH)₂; (2) dissolution of the Ni(OH)₂; (3) reduction of the dissolved Ni(OH)₂ by hydrazine; (4) nucleation and growth of the nickel particles from the ethylene glycol solution onto the surfaces of the Al particles. The reactions took place according to the following equations:

$$Ni(Ac)_2 + 2NaOH \rightarrow Ni(OH)_2 + 2NaAc \qquad (1)$$

$$Ni(OH)_2 + (1/2)N_2H_4 \rightarrow Ni + (1/2)N_2 + 2H_2O \qquad (2)$$
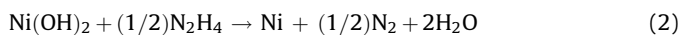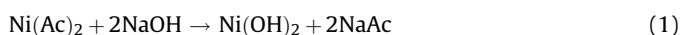
This modified polyol method requires a low-processing temperature of 60 °C. This is much lower as compared to conventional polyol process which requires the reaction to occur at the boiling temperature of polyol (~200 °C) [11,12]. Moreover, the by-products (N₂ and H₂O) are environmentally friendly and can be easily removed.

NaOH plays an important role in this process. The first role of NaOH is to allow Ni(OH)₂ to precipitate from the Ni(Ac)₂. The second role of the alkali is to provide sufficient alkalinity for the use of the hydrazine as an effective reducing agent. Lastly, NaOH also serves to remove some of the thin alumina layer present on the Al surface before depositing the Ni nano-particles. NaOH may act as a strong alkali and can help to "dissolves" away the alumina oxide layer. The synthesis process was done in a flask reactor flushed with a continuous flow of nitrogen. It was not done in an inert condition thus aluminum is consistently being oxidized throughout the process. The reaction involved is as shown:

$$Al_2O_3(s) + 2NaOH(aq) + 3H_2O(l) \rightarrow 2Na^+(aq) + 2[Al(OH)_4]^-(aq) \qquad (3)$$
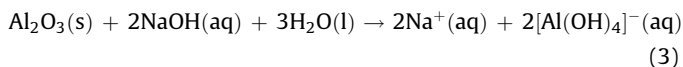
The powders obtained were characterized using various techniques. A scanning electron microscope (SEM) (JEOL JSM-6360A) was used to analyze the size and morphology of the powders. The SEM is equipped with energy dispersive X-ray spectrometer (EDX) that allows elemental analysis. The X-ray diffraction patterns of the powders were obtained with a Shimadzu 6000 X-ray Diffractometer (XRD) using a Cu target ($\lambda_{Cu\ K\alpha}$ = 1.5405 Å). Differential scanning calorimetric (DSC) and thermogravimeteric analysis (TGA) were done in purified air using the TA instruments SDT 2960 Simultaneous DSC-TGA to study the thermal properties of the samples. The sample was ramped from room temperature to 1400 °C at a heating rate of 20 °C/min in purified air.

3. Results and discussion

Ni particles synthesized in a blank run, without the addition of the Al powders, is shown in Fig. 1. Nano-sized (~100–200 nm) Ni particles, which were spherical and uniform in shape, were obtained using the modified polyol process. With the addition of the Al powders, Ni-coated Al powders were obtained, and the morphology of the coated powders is shown in Fig. 2(a)–(c). The nano-sized Ni particles are clearly seen deposited onto individual
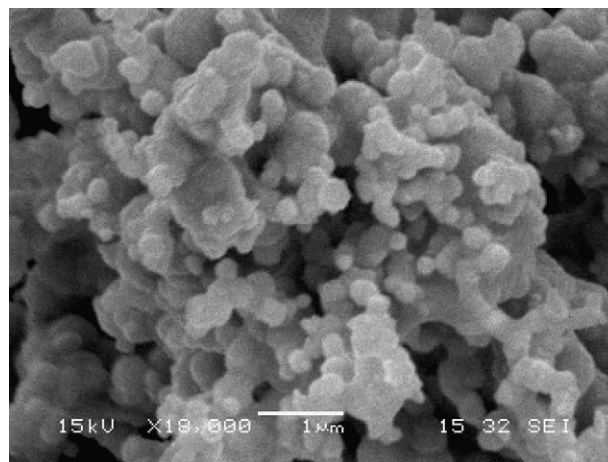

Fig. 1. SEI micrographs of as-prepared Ni particles.

Al particles. The coating process is proposed to occur not only by pure adhesion of Ni nanoparticles onto the Al surface but also nucleation of Ni particles from the Al particles itself. Upon reaching super saturation, precipitation of nickel particles occurred and the presence of Al particles acts as sites for heterogeneous nucleation of nickel to take place. The coating mechanism is proposed to occur more favorably at the grain boundaries since thermodynamically, lower activation energy is required. However, it is also possible for homogenous precipitation of nickel to occur in the solution and to subsequently physical adhere to the surface. During the process, the solution was mechanically stirred at 400 rpm. This mechanically stirring process can generate new grain boundaries and defects which can enhance the nucleation of Ni particles from Al. This can eventually lead to a more uniform coating. EDX elemental mapping was also done to further confirm that a fairly uniform coating was achieved. However, it should be noted that the Ni coating is not in the form of a uniform shell. There will still be some portion of Al particle that are exposed and an oxide layer will still exist in regions where there is no Ni coating.

XRD spectra of the coated powders of various bulk compositions are shown in Fig. 3. All the diffraction peaks correspond to the pure elemental Al and Ni phases. No additional peaks corresponding to secondary phases were observed. This indicates that only the coating of Ni onto Al particles took place, and no Al–Ni intermetallic phases were formed during the synthesis process. It is also noted that the diffraction peaks corresponding to Ni are broader than those corresponding to Al. The nickel particles have an average diameter of ~100 nm compared to Al of ~50 μm. Hence, the difference in peak broadness indicates the crystalline size difference between the micron-sized Al particles and nano-sized Ni coating.

Thermal analysis was performed on the Ni-coated Al powders using TGA and DSC. The study of the thermal behavior of the powders in air provides a good indication of the combustion behavior of the Al powders, since combustion is an oxidation process. The onset temperature, defined as the temperature at which the first oxidation commenced, can be taken to be the temperature where a first sharp increase in weight gain is registered in the TGA curve. This onset TG temperature can be used to indicate the ease of ignition of the Al-based powders. TG onset can serve as one of the parameters of measurement for the reactivity in air as reported by Ilyin et al. [13]. It was also mentioned that the TG onset could be used to reflect the reactivity of Al-metal system. Hahma et al. [14] also made a study on the ignitability of different Al-metal/organic coatings and concluded that the lower the temperature of the first strong exotherm, the better is the ignitability.
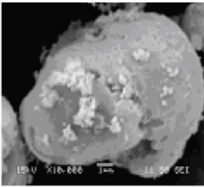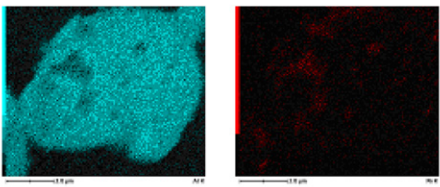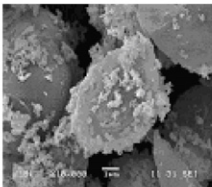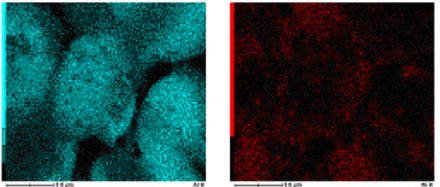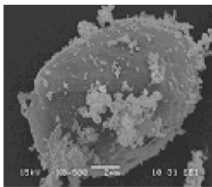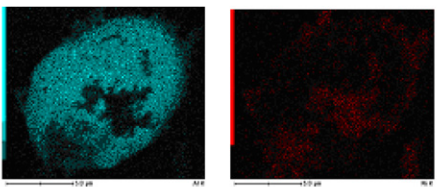
Fig. 2. SEI and EDX images of (a) 5 wt% Ni–Al; (b) 10 wt% Ni–Al; (c) 30 wt% Ni–Al.

A comparison of the TGA curves obtained for the as-synthesized Ni nanoparticles and a commercially available Ni powders (Alfa Aesar, 100 mesh, particle size of ~150 μm) is provided in Fig. 4. It is obvious that the oxidation of the Ni particles synthesized using the modified polyol process took place at a much lower temperature (~317 °C) than that of the pure commercial Ni powders (~567 °C). The early TG onset was due to the nano-sized powders having a larger specific surface area and thus hasten the oxidation process. It is also noted that there is an initial decrease in weight for the polyol synthesized Ni sample. This is due mainly to the vaporization of absorbed species such as moisture or other organic species.

The TGA curves, showing the respective sample mass increase as a function of temperature, obtained for the pure untreated Al and Ni-coated Al powders at a heating rate of 20 °C/min are shown in Fig. 5(a) and (b). For pure Al powders, four distinct stages were observed, and the oxidation mechanism is in accordance to that proposed by Trunov et al. [15]. It was proposed that during stage 1, from 600 to 650 °C, the process first involves the formation of the amorphous alumina and then conversion into the γ-Al$_2$O$_3$. The thickness of the natural amorphous alumina layer increases and when it exceeds the critical thickness of amorphous alumina layer of 4 nm, it transforms into γ-Al$_2$O$_3$. The rate of this process increases rapidly at the onset and decreases as the γ-Al$_2$O$_3$
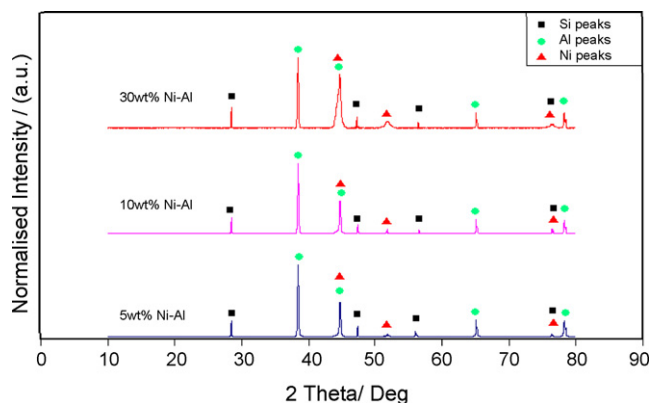

Fig. 3. X-ray diffraction patterns of different wt% Ni-coated Al samples. Si was added as an internal reference.

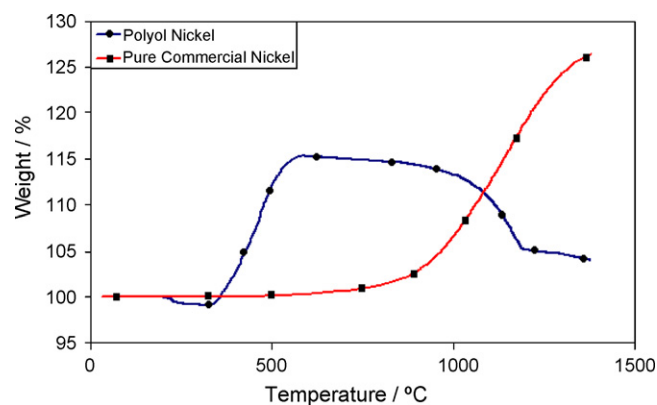**Fig. 4.** TGA graphs of Ni nanoparticles prepared by modified polyol process and commercially available Ni micron-sized particles.

Table 1
Comparison of the TG onset of untreated Al powders, the different wt% Ni-coated Al powders and pure Ni nanoparticles synthesized using the modified polyol process

Sample	TG onset (°C)
Untreated pure Al	607
5 wt% Ni-coated Al	417
10 wt% Ni-coated Al	403
30 wt% Ni-coated Al	347
As-synthesized Ni nanoparticles	317

For the Ni-coated Al powders, four distinct stages similar to pure Al were still observed, except that the onset temperature of the first oxidation process (stage 1) occurs at a much lower temperature. For stage 1, it is the oxidation of nickel that is taking place, and this occurs at temperatures ranging from 350 to 420 °C for the Ni-coated Al powder samples. The onset is close to the value observed for the pure Ni particles obtained in the blank run (Fig. 4). The presence of the nano-sized nickel particles lowered the overall onset of oxidation to a much lower temperature (stage 1) as compared to pure untreated Al. Upon reaching stage 2, the Ni particles were more or less being completely oxidized. This is supported by the TGA graph for pure Ni particles in Fig. 4, showing a plateau upon reaching ~600 °C.

The onset TG temperatures obtained from the TGA curves for all the samples are summarized in Table 1. It is observed that the TG onset for Ni-rich samples (30 wt% Ni) is lower than the Al-rich samples (5 and 10 wt% Ni). Oxidation of nano-sized Ni particles occurred at a much lower temperature as compared to the micron-sized Al particles. With increasing Ni content, oxidation of Ni becomes the dominating process compared to the conversion of amorphous Al_2O_3 to γ-Al_2O_3 during this stage thus lowering the TG onset.

Fig. 5(c) shows the DSC graphs of the different composition of Ni-coated Al powders together with the untreated Al powders. It is observed that the powders first undergo a solid-state energy released which corresponds to the stage 1 oxidation shown in the TGA graphs. It is noted that the energy released for the Ni-rich sample (30 wt% Ni) is much higher than the Al-rich samples (5 and 10 wt% Ni) for this exotherm. The larger enthalpy produced in the first exotherm is mainly due to the oxidation of Ni to NiO which is the main oxidation step as compared to the oxidation of Al in Al-rich samples. This is in good agreement with a higher rate of oxidation for Ni-rich samples in the stage 1 observed in the TGA graphs. Oxidation of Ni occurs at a faster rate compared to Al due to its nano-size, which contributes to larger effective surface area. Moreover, oxidation of Al is hindered by the formation of the non-porous oxide layer. Thus, the ease of Ni oxidation contributed to the larger enthalpy released shown in the first exotherm.

The second exotherm corresponds to stage 3 shown in the TGA curves. This stage mainly involves the breakage of the alumina layer followed by the rapid oxidation of the exposed active Al. The general oxidation enthalpy of the second exotherm is observed to be larger in the Al-rich powders (5 and 10 wt% Ni) than the Ni-rich (30 wt% Ni) powders. This is mainly due to the fact that Al has a higher specific enthalpy than Ni. However, it is interesting to note that the 10 wt% Ni-coated Al sample has the largest enthalpy during this stage, although the Al content is lower as compared to the 5 wt% Ni sample. This is also consistent with the TGA results shown in Fig. 5(b) whereby the 10 wt% Ni sample has the fastest rate of oxidation during this stage. A possible explanation for this is that the 10 wt% Ni-coated Al powders have the most optimum amount of coating among the samples. This may reduce agglomeration of the melted Al, and thus contributing to more active Al for combustion. Hence, it can be concluded that the
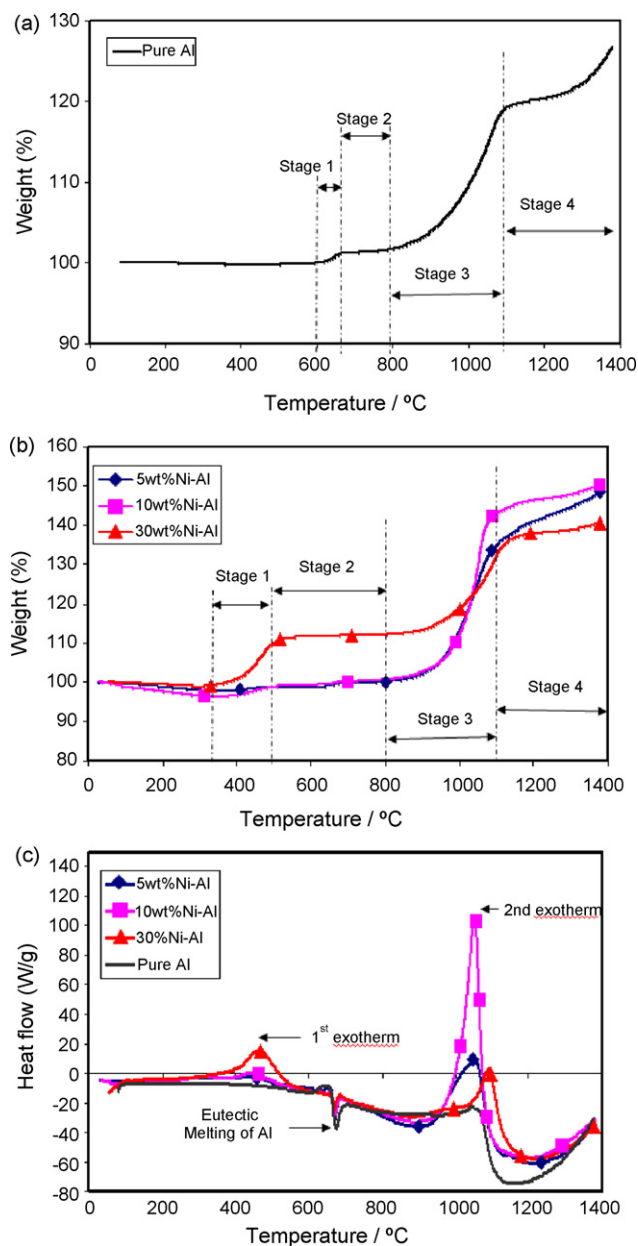
Fig. 5. TGA graphs of (a) pure untreated Al powders and (b) different wt% Ni-coated Al powder samples; (c) DSC curves of different wt% Ni-coated Al powder samples.

becomes thicker and more continuous. This process corresponds to the oxide skin on the particles thickening and provides a kinetic barrier to further weight gain. Stage 2 (650 °C to about 800 °C) is mainly dominated by the oxidation of γ-Al_2O_3 and is distinguished by a flat plateau with minimal weight change as oxidation is relatively slow and limited by the diffusion of oxygen atoms through the thick Al_2O_3 layer. The oxidation rate increases rapidly at the onset of stage 3 due to the eventual cracking of the thick alumina layer leading to rapid diffusion of oxygen through the cracks towards the Al/Al_2O_3 interface. A sudden increase in oxidation of Al leads to a rapid weight change during this stage. This layer of Al_2O_3 is characterized as the θ-Al_2O_3 polymorph. Finally, stage 4 is observed for the transition from θ-Al_2O_3 to the stable α-Al_2O_3. This process results in an abrupt reduction in the oxidation rate due to the formation of significantly denser and coarser crystallites of α-Al_2O_3, which reduces the rate of oxygen diffusion and resulting in slower alumina growth rate.
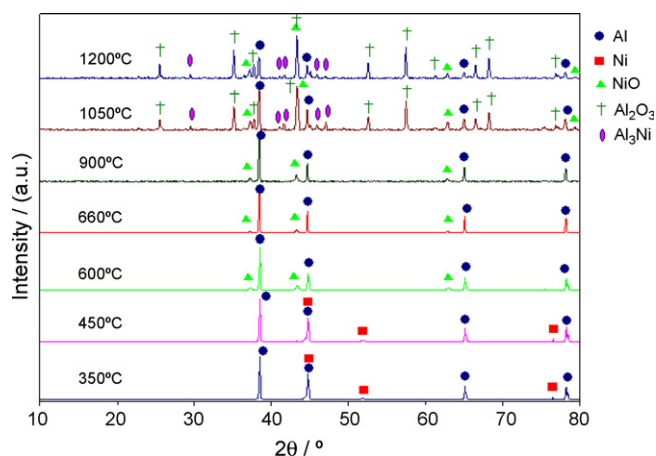
Fig. 6. X-ray diffraction patterns for the 10 wt% Ni–Al post-TGA samples at different temperature demonstrating the formation of the intermetallic product, NiAl$_3$ from 1050 °C onwards.

enthalpy of the second exotherm depends not only on the composition but also the amount of Ni coating onto the Al powders.

In order to get a better understanding on the phase changes upon heating, XRD analyses were also performed on the samples heated at various temperatures to determine the combustion products of the reaction. The temperatures were chosen based on the TGA results. The temperatures chosen are the onset of mass increase; point of inflection and the point whereby the final plateau has reached (where oxidation was more or less completed). The samples at the selected temperatures were prepared by heating the powders at room temperature to the temperature required at a heating rate of 20 °C/min in the DSC followed by subsequent cooling to room temperature and analysis using the XRD. Fig. 6 shows the X-ray diffraction patterns of the 10 wt% Ni–Al sample obtained at the various different temperatures. Prior to reaching 600 °C, all the peaks correspond to the as-synthesized powder. No additional phases were detected Diffraction peaks corresponding to NiO phase were only detected in samples heated to 600 °C and above. However, the onset of oxidation as determined from TGA occurred at a much lower temperature. This difference may be due to the formation of the amorphous phase NiO first prior to the formation of the crystalline NiO phase. Further thermal treatment to 1050 °C and above resulted in the gradual formation of two additional phases; α-phase aluminum oxide and an intermetallic compound, Al$_3$Ni. According to Philpot et al. [16], the reaction proceeds at around 640 °C and involves the

solid-state diffusion of Ni atoms in Al according to the following equation:

$$3Ni + Al \rightarrow NiAl_3$$

However, this temperature can only be used as a reference as it uses a different synthesis method; combustion synthesis to produce the intermetallic.

Rietveld analysis was done on the XRD pattern for the sample heated to 1200 °C. The final combustion product consists of 13.7 wt% Al, 72.4 wt% Al$_2$O$_3$, 7.0 wt% NiO and 6.9 wt% Al$_3$Ni. The bulk weight of the combustion product was mainly contributed by the α-phase alumina with the intermetallic; NiAl$_3$ forming the minor phase.

4. Conclusions

This work investigates the deposition of nanocrystalline nickel particles on micron-sized Al powders using a modified polyol process. Different compositions of Ni-coated Al powders were successfully synthesized. The oxidation kinetics of the coated powders was significantly improved as compared to untreated Al powders. Other than the oxides, the intermetallic Al$_3$Ni phase was also detected in the combustion products heated to 1050 °C and above.

Acknowledgements

References

[1] E.W. Price, in: K. Kuo, M. Sommerfield (Eds.), Progress in Aeronautics and Astronautics, AIAA, New York, 1984, p. 479.
[2] E.W. Price, R.K. Sigman, in: V. Yang, T.B. Brill, W.Z. Ren (Eds.), Progress in Aeronautics and Astronautics, AIAA, Reston, VA, 2000, p. 663.
[3] A.L. Breitler, V.M. Mal'tsev, E.I. Popov, Combust. Explos. Shock Waves 26 (1988) 86.
[4] V.A. Babuk, V.A. Vassiliev, V.V. Sviridov, Combust. Sci. Technol. 163 (2001) 261.
[5] D.A. Yagodnikov, A.V. Voronetskii, Combust. Explos. Shock Waves 33 (1997) 49.
[6] L. Thiers, A.S. Mukasyan, A. Varma, Combust. Flame 131 (2002) 198.
[7] E. Shafirovich, P.E. Bocanegra, C. Chauveau, I. Gökalp, U. Goldshleger, V. Rosenband, A. Gany, Proc. Combust. Inst. 30 (2005) 2055.
[8] Z. Jiang, S. Li, F. Zhao, Z. Liu, C. Yin, Y. Luo, S. Li, Propell. Explos. Pyrotechnol. 31 (2006) 139.
[9] Y. Kening, D.J. Kim, H.S. Chung, H. Liang, Mater. Lett. 57 (2003) 3992.
[10] S. Wu, D. Chen, J. Colloid Interf. Sci. 259 (2003) 282.
[11] L.K. Kurihara, G.M. Chow, P.E. Schoen, Nanostruct. Mater. 5 (1995) 607.
[12] Y. Zhou, S. Jin, G. Qiu, M. Yang, Mater. Sci. Eng. B 122 (2005) 222.
[13] A. Ilyin, A. Gromov, V. An, Propell. Explos. Pyrotechnol. 27 (2002) 361.
[14] A. Hahma, A. Gany, K. Palovuori, Combust. Flame 145 (2006) 464.
[15] M.A. Trunov, M. Schoenitz, X. Zhu, E.L. Dreizin, Combust. Flame 140 (2005) 310.
[16] K.A. Philpot, Z.A. Munir, J.B. Holt, J. Mater. Sci. 22 (1987) 159.